Algorithm Theoretical Basis Document (ATBD)

(Ver.1.1)

GSICS Inter-calibration of INSAT-3D Imager and Sounder infrared channels using Metop-A IASI Hyperspectral Observations

P K Thapliyal, M V Shukla, Ipshita Dey and Shivani Shah

Space Applications Centre
Indian Space Research Organisation (ISRO)
Ahmedabad (INDIA)

The INSAT-3D satellite was launched by India Space Research Organisation (ISRO) on 26 August 2013 in a geostationary orbit located at 82E over Indian Ocean. INSAT-3D has two instruments, namely Imager and Sounder, for continuous meteorological observations over Indian Ocean region. The imager makes full disk observations every 30 minutes at 6 channels, whereas the Sounder makes observations at 18 infrared channels (plus a visible channel for cloud detection during daytime) at the interval of an hour. The Imager has spatial resolutions of 1 km for visible (VIS) and shortwave infrared (SWIR) channels, 4 km for mid-wave infrared (MIR) and split window thermal infrared (TIR1 & TIR2) and 8 km for the water vapour absorption channel (WV) at nadir. The Sounder makes observations at a spatial resolution of 10 km at nadir.

This document describes the theoretical basis of an algorithm that guides the series of processes for a specific inter-calibration of the Infrared sensors onboard Indian geostationary satellites such as INSAT-3D using hyperspectral observations from the state-of-the-art Infrared Atmospheric Sounding Interferometer (IASI) onboard Low Earth Orbiting (LEO) satellite MetOp-A. The algorithm has been adopted from standard GSICS algorithm (Hewison et al., 2013; and suitably modified for specific INSAT-3D satellite and has been implemented at SAC/ISRO. The goal of this inter-calibration is to make INSAT-3D measurements traceable to IASI.

The Atmospheric InfraRed Sounder (AIRS) onboard EOS-Aqua and IASI are used widely as the reference instrument for the inter-calibration. These two LEO hyperspectral instruments are chosen as references in the GSICS GEO-LEO inter-calibration due to the following reasons: (1) radiances of these two instruments are highly calibrated due to the advanced pre-launch and on-board radiometric and spectral calibrations (Pagano et al. 2003, Blumstein et al. 2007), (2) spectral and radiometric calibrations of both instruments are very stable since on-orbit (Pagano et al. 2003, Blumstein et al. 2007), (3) the band-to-band radiometric calibration difference between the two instruments is very small within less than 0.1K difference (Strow et al. 2008, Tobin 2008, Elliot et al. 2009); (4) the hyperspectral measurements can be easily transformed to the pseudo broad channels for the senor-to-sensor inter-calibration (Tobin et al., 2006, Tahara and Kato, 2009; Shukla et al., 2012); and (5) the mean Tb difference of these two hyperspectral Sounder at broad wavelengths is less than 0.1K [Wang et al. 2011], providing more opportunities to monitor the GEO operational

calibration and detect the calibration anomaly with two pairs of satellite collocation data.

This document is constructed under a hierarchical structure for all inter-calibrations, in particular for all inter-calibrations between INSAT-3D and IASI. This hierarchical structure was proposed by the GSICS Data Working Group (GDWG) (November 2009) and adopted by the GSICS Research Working Group (GRWG). It defines the following generic steps:

1) Subsetting
2) Collocating
3) Transforming
4) Filtering
5) Monitoring
6) Correcting

Each step comprises a number of discrete components; each component is defined in the following hierarchical way:

i. Describe the purpose of this component
ii. Provide options for how these may be implemented in general.
iii. Recommend procedures for the inter-calibration class (e.g. GEO-LEO).
iv. Provide specific details for each instrument pair (e.g. INSAT-3D Sounder and Imager with IASI).

Each component is defined independently and may exist in different versions. The implementation of the algorithm need only follow the overall logic – so the components need not be executed strictly sequentially. For example, some parts may be performed iteratively, or multiple components may be combined within a single loop in the code.

GSICS aims to define a "baseline" algorithm by identifying one version of each component, against which the performance of other versions may be compared.

1. Subsetting

First step is to perform a rough cut to reduce the data volume and only include relevant portions of the dataset (channels, area, time, viewing geometry). The purpose is to select portions of data collected by the two instruments that are likely to produce collocations. This is desirable because typically less than 0.1% of measurement is collocated. The processing time is reduced substantially by excluding measurements unlikely to produce collocations.

For inter-calibrations between geostationary and sun-synchronous satellites, the orbits provide collocations near the GEO Sub-Satellite Point (SSP) within fixed time windows every day and night. *We define the GEO Field of Regard (FoR) as an area close to the GEO Sub-Satellite Point (SSP), which is viewed by the GEO sensor with a zenith angle less than a threshold*. Wu [2009] defined a threshold angular distance from nadir of less than 60° based on geometric considerations, which is the maximum incidence angle of most LEO sounders. This corresponds to ≈ 52° from the GEO SSP. The GEO and LEO data is then subset to only include observations within this FoR within each inter-calibration period.

1.a.i. **INSAT-3D - IASI Specific** (trial and error basis)

Each IASI granule is compared with each INSAT-3D images in the input data. Only the pairs that are possible to produce collocations (collocated in space and sufficiently close in time) are retained for further analysis. We extract the IASI granules in the region 30-120E, 45S-45N for further processing.

Entire IASI orbit is divided into small granules of 3 minutes to make the search faster.

2. Find Collocations

A set of observations from a pair of instruments within a common period (1 day) is required as input to the algorithm. The first step is to obtain these data from both instruments, select the relevant comparable portions and identify the pixels that are spatially collocated, temporally concurrent, geometrically aligned and spectrally compatible and calculate the mean and variance of these radiances.

2.a. *Collocation in Space*

2.a.i. Purpose

First we extract the central location of each instruments' pixels and determine which pixels is considered to be collocated, based on their centres being separated by less than a pre-determined threshold distance. At the same time we identify the pixels that define the *target area* (FOV) and *environment* (ENV) around each collocation.

The *target area* is defined to be a little larger than the larger Field of View (FoV) of the two instruments so it covers all the contributing radiation in event of small navigation errors, while being large enough to ensure reliable statistics of the variance are available. *The exact ratio of the target area to the FoV will be instrument-specific, but in general will range 1 to 3 times the FoV, with a minimum of 9 'independent' pixels.*

2.a.ii. Infrared GEO-LEO inter-satellite/inter-sensor Class

The spatial collocation criterion is based on the nominal radius of the LEO FoV at nadir. This is taken as a threshold for the maximum distance between the centre of the LEO and GEO pixels for them to be considered spatially collocated. However, given the geometry of the already subset data, it is assumed that all LEO pixels within the GEO FoR will be within the threshold distance from a GEO pixel.

2.a.iii. INSAT-3D - IASI Specific: For INSAT-3D Imager we take 5 x 5 pixels for MIR, TIR1 and TIR2 channels, 3 x 3 pixels for WV channel as the target area, whereas for Sounder we take 3 x 3 pixels as target area centred at IASI pixel centre. This fulfils the criteria of maintaining a minimum of 9-pixel for target area.

2.b. *Concurrent in Time*

Next we need to identify which of those pixels identified in the previous step as spatially collocated are also concurrent in time. Although even collocated measurements at very different times may contribute to the inter-calibration, if treated properly, the capability of processing collocated measurements is limited and the more closely concurrent ones are more valuable for the inter-calibration.

Each pixel identified as being spatially collocated is tested sequentially to check whether the observations from both instruments were sampled sufficiently closely in

time – i.e. separated in time by no more than a specific threshold. This threshold should be chosen to allow a sufficient number of collocations, while not introducing excessive noise due to temporal variability of the target radiance relative to its spatial variability on a scale of the collocation target area [Hewison, 2009]

The time at which each collocated pixel of the INSAT-3D Image and Sounder were sampled are extracted or calculated and compared to the collocated IASI pixel. If the difference is greater than a threshold of 300s, the collocation is rejected; otherwise it is retained for further processing.

$$| LEO\_time - GEO\_time | < max\_sec, \qquad \text{where, max\_sec=300s}$$

2.b.i. INSAT-3D - IASI Specific: IASI time is read from the data and INSAT-3D Imager and Sounder time is calculated from the scan-line time information provided with the dataset. In order to find sufficient number of matchup dataset the threshold *max_sec* is increased to 15 minutes for INSAT-3D Sounder due to its smaller coverage area, whereas it is retained as 5 minutes for Imager that is available at full disk.

2.c. *Alignment in Viewing Geometry*

2.c.i. Purpose

The next step is to ensure the selected collocated pixels have been observed under comparable conditions. This means they should be aligned such that they view the surface at similar incidence angles. The criterion for zenith angle is defined in terms of atmospheric path length, according to the difference in the secant of the observations' zenith angles and the difference in azimuth angles. If these are less than pre-determined thresholds the collocated pixels can be considered to be aligned in viewing geometry and included in further analysis, otherwise they are rejected.

Stringent criterion on the viewing zenith angle is applied for the geometric alignment of infrared GEO-LEO inter-calibration.

$$\left| \frac{\cos(geo\_zen)}{\cos(leo\_zen)} - 1 \right| < \max\_zen$$

The threshold value for max_zen can be quite large for window channels (e.g., 0.05 for 10-12 μm channels) but must be rather small for more absorptive channels (e.g., <0.02 for 7 or 14 μm channel). Unless there are particular needs to increase the sample size for window channels, a common threshold value of *max_zen* = 0.01 is recommended for all channels. This results in collocations being distributed approximately symmetrically about the equator mapping out a characteristic *slanted hourglass* pattern.

Another aspect of viewing geometry alignment is azimuth angle. Similar zenith angle assures similar path length; additional requirement of similar azimuth angle assures similar line-of-sight. Line-of-sight alignment is relevant for IR spectrum in certain cases. For infrared window channels, land surface emission during daytime may be anisotropic [Minnis et al. 2004]. For shortwave IR band (e.g., 4 μm), azimuth angle alignment is required during daytime when solar radiation is considerable. It is, therefore recommended that inter-calibration over land and in this band is limited to night-time only cases – at the expense of limiting the dynamic range of the results.

Fig.1 shows a sample collocation map after spatial and temporal collocation of INSAT-3D Sounder and Imager with IASI.

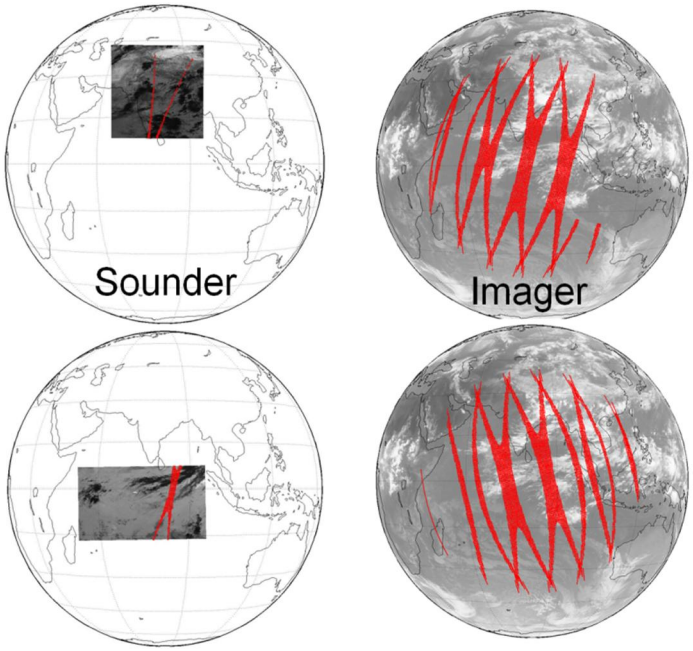

Fig.1: Sample collocation maps of INSAT-3D Imager/Sounder with Metop-IASI

2.c.ii. INSAT-3D - IASI Specific: The value of *max_zen* is kept 0.01 for both Imager and Sounder. We use only night-time data to avoid the difference arising due to the viewing geometry or azimuth angle. Day-time data is also processed but will be used only for research purpose and to monitor the diurnal variation in the instrument calibration.

2.d. *Pre-Select Channels*

2.d.i. Purpose

Only broadly comparable channels from both instruments are selected to reduce data volume.

2.d.ii. Infrared GEO-LEO inter-satellite/inter-sensor Class

Only the channels of the GEO and LEO sensors are selected in the thermal infrared range of 3-15µm.

2.d.iii. INSAT-3D - IASI Specific: Select the four Imager and 18 Sounder infrared channels for INSAT-3D with central wavelength longer than 3µm. The fig.2 (a

& b) show INSAT-3D SRFs for Sounder and Imager, respectively, overlaid on IASI spectra.

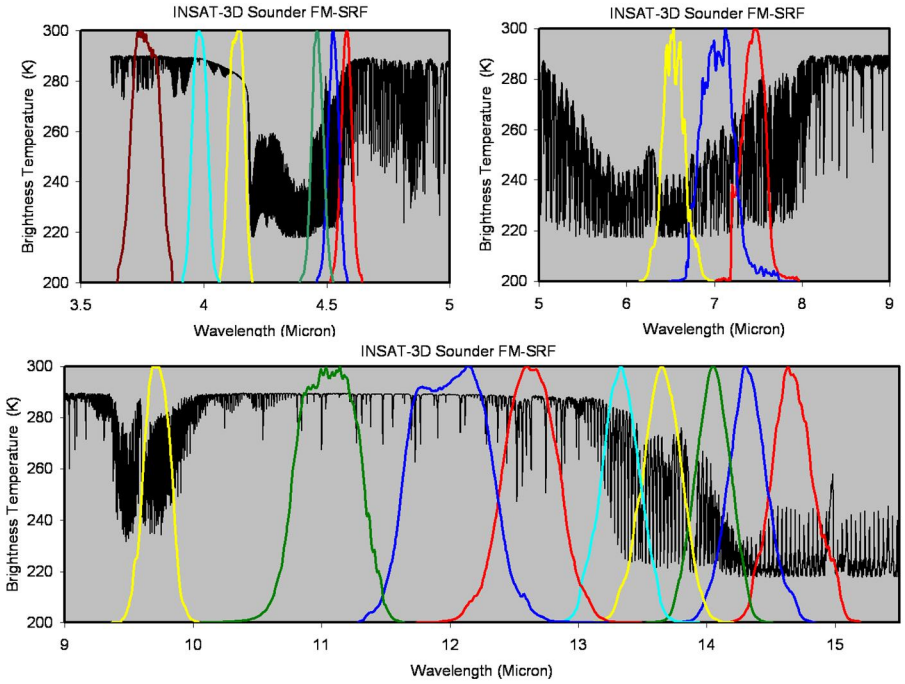

Fig.2a: INSAT-3D Sounder SRFs overlaid on IASI spectrum

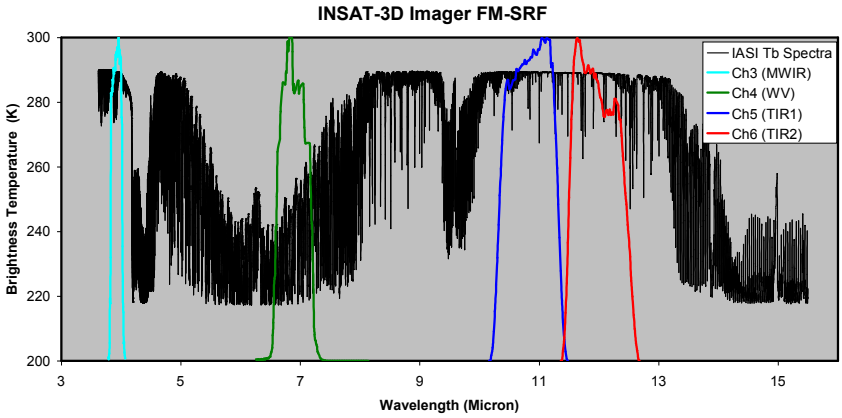

Fig.2b: INSAT-3D Imager SRFs overlaid on IASI spectrum

2.e. *Plot Collocation Map*

2.e.i. Purpose

When interpreting the inter-calibration results it is often helpful to visualise the distribution of the source data used in the comparison.

2.e.ii. General Options

This can be achieved by producing a map showing the distribution of collocation targets.

2.e.iii. Infrared GEO-LEO inter-satellite/inter-sensor Class

The map is produced showing all the GEO-LEO pixels meeting the collocation criteria every day. These points are overlaid on a background image from an infrared window channel of the GEO instrument. This allows the distribution of cloud to be visualised and considered in the interpretation of the results.

2.e.iv. INSAT-3D - IASI Specific

Collocation maps for Imager and Sounder are generated daily as shown in Fig.1.

3. Transform Data

In this step, collocated data are transformed to allow their direct comparison. This includes modifying the spectral, temporal and spatial characteristics of the observations, which requires knowledge of the instruments' characteristics. The outputs of this step are the best estimates of the channel radiances, together with estimates of their uncertainty.

3.a. *Convert Radiances*

Convert observations from both instruments to a common definition of radiance to allow direct comparison. Comparisons are performed in radiance units, $mW/m^2/st/cm^{-1}$.

3.b. *Spectral Matching*

First, we must identify which channel sets provide sufficient common information to allow meaningful inter-calibration. These are then transformed into comparable pseudo channels, accounting for the deficiencies in channel matches.

The Spectral Response Functions (SRFs) must be defined for all channels. The observations of channels identified as comparable are then co-averaged using pre-determined weightings to give *pseudo channel* radiances. A Radiative Transfer Model can be used to account for any differences in the pseudo channels' characteristics. The uncertainty due to spectral mismatches is then estimated for each channel.

For hyper-spectral instruments, all SRFs are first transformed to a common spectral grid. The LEO hyperspectral channels are then convolved with the GEO channels' SRFs to create synthetic radiances in pseudo-channels, accounting for the spectral sampling and stability in an error budget.

$$R_{GEO} = \frac{\int_{\nu} R_{\nu} \Phi_{\nu} d\nu}{\int_{\nu} \Phi_{\nu} d\nu}$$

where, R_{GEO} is the simulated GEO radiance, R_{ν} is LEO radiance at wavenumber ν, and Φ_{ν} is GEO spectral response at ν.

In general LEO hyperspectral sounders do not provide complete spectral coverage of the GEO channels either by design (e.g. gaps between detector bands), or by subsequent hardware failure (e.g. broken or noisy channels). The radiances in these *gap channels* shall be accounted using a proper techniques.

3.b.i. INSAT-3D - IASI Specific:

The IASI channels are assumed to be spectrally stable. INSAT-3D Imager and Sounder SRFs are linearly interpolated onto IASI spectral grid in the wavenumber-space. Any negative responses in the interpolated SRFs are set to zero and then the interpolated SRFs are normalized to [0, 1]. The gap channels in IASI due to bad quality flags are filled using linear interpolation from nearby channels. So far IASI has produced complete spectrum without any missing/bad-channels.

3.c. *Spatial Matching*

The observations from each instrument are transformed to comparable spatial scales. This involves averaging all the pixels identified within the *target* and *environment* areas. The uncertainty due to spatial variability is estimated.

3.c.i. Infrared GEO-LEO inter-satellite/inter-sensor Class

The *target area* is defined as a GEO array (and 3 x 3 pixels for Sounder in INSAT-3D) with the nominal LEO FoV at nadir centred at the GEO pixel which is the closest to the centre of the collocated LEO pixel. The *target area* is considered the pseudo GEO pixel at LEO nominal spatial resolution. The GEO pixels within target area are averaged using a uniform weighting and their variance is calculated. The *environment* is defined by the GEO pixels within 4x radius of the target area from the centre of each collocated LEO FoV.

3.c.ii. INSAT-3D - IASI Specific:

For INSAT-3D Imager the *target* area is an array of 5 x 5 pixels for Imager MIR, TIR1 and TIR2 channels, and 3 x 3 pixels for WV channel. The *environment* is an array of 15x15 pixels for MIR, TIR1 and TIR2, and 7x7 pixels for WV channel to make it symmetrical around centre of the target pixel.

For INSAT-3D Sounder the *target* area is an array of 3x3 pixels and the *environment* is an array of 7x7 pixels to make it symmetrical around centre of the target pixel.

3.d. *Viewing Geometry Matching*

Despite the collocation criteria described above, each instrument can measure radiance from the collocation targets in slightly different viewing geometry. It may be possible to account for small differences by considering a simplified radiative transfer model. Differences in viewing geometry within the collocation criteria described here are assumed to be negligible and ignored in further analysis.

3.d.i. INSAT-3D - IASI Specific

Viewing geometry differences are ignored in this case.

3.e. *Temporal Matching*

Different instruments measure radiance from the collocation targets at different times. The impact of this difference can usually be reduced by careful selection, but not completely eliminated. The timing difference between instruments' observations is established and the uncertainty of the comparison is estimated based on (expected or observed) variability over this timescale.

3.e.i. INSAT-3D - IASI Specific

Only the INSAT-3D observations closest to the IASI equator crossing time are selected. The time difference between the collocated GEO and LEO observations is neglected and the collocation targets are assumed to be sampled simultaneous, contributing no additional uncertainty to the comparison.

4. Filtering

The collocated and transformed data will be archived for analysis. Before that, the GSICS inter-calibration algorithm reserves the opportunity to remove certain data that should not be analyzed (quality control), and to add auxiliary data that will add further analysis. For example, it may be useful to incorporate land/sea/ice masks and/or cloud flags to better classify the results.

4.a. *Time Selection*

4.a.i. Purpose

The collocation data may range a few hours every day and night. The effects of stray-light at all GEO instruments and the erroneous midnight calibration responsibility of the three-axis stabilized GEO satellite can result in time-dependent degraded GEO radiance. It is therefore necessary to select the optimal time period in a day to maximally reduce the inter-calibration accuracy uncertainty.

4.a.ii. INSAT-3D - IASI Specific:

For IASI as reference instrument night-time collocation data before the significant impact of erroneous midnight calibration responsivity (10:00PM at satellite local time) will used for the INSAT-3D intercalibration.

4.b. *Uniformity Test*

Knowledge of scene uniformity is critical in reducing and evaluating inter-calibration uncertainty. To reduce uncertainty in the comparison due to spatial/temporal mismatches, the collocation dataset may be filtered so only observations in homogenous scenes are compared.

4.b.i. General Options

i) The simplest option is to allow all inter-calibration targets, regardless of their uniformity.

ii) Another option is to set threshold to allow only relatively uniform scenes for analysis. In this case, the spatial/temporal variability of the scene within the target area is compared with pre-defined thresholds to exclude scenes with greater variance from analysis. This may be performed on a per-channel basis.

iii) Another option is to use scene uniformity as weight in further analysis. Comparatively, the threshold option has the theoretical disadvantage of subjectivity but practical advantage of substantially reducing the amount of data to be archived.

4.b.ii. INSAT-3D - IASI Specific:

We have used both (4.b.ii) and (4.b.iii) by using variance of the target pixels as weights and excluding collocated data above a relatively high threshold scene variance (*environment pixels*) as discussed in (4.c.i).

4.c. *Outlier Rejection*

Purpose

To prevent anomalous observations having undue influence on the results, 'outliers' may be identified and rejected on a statistical basis. Small number of anomalous pixels in the environment, even concentrated, may not fail the uniformity test. However, if they appear only in one sensor's field of view but not the other, it can cause unwanted bias in a single comparison.

4.c.i. INSAT-3D - IASI Specific

All inter-calibration targets are included in further analysis, regardless of whether they are outliers with respect to their environment.

Only exception: The mean GEO radiances within each LEO FoV are compared to the mean of their *environment*. Targets where this difference is >3 times the standard deviation of the environment's radiances are rejected. The following additional checks were applied to remove the satellite acquisitions that has large geolocation/quality error or spurious data:

- Difference of IASI convolved INSAT-3D radiances and actual INSAT-3D radiance ($\Delta R = R_{IASI} - R_{INSAT3D}$) are computed for individual granule/satellite acquisition. Median (M) of this difference, ΔR, is computed for the entire granule/acquisition. The median absolute deviation (MAD) is computed for each granule/acquisition ($MAD = median\{abs(\Delta R - M)\}$). If any collocation pair in the given granule has difference more than ±3*MAD then it is considered as an outlier.
- After this check we compute statistics between R_{IASI} and $R_{INSAT3D}$ for each granule/ acquisition, such as coefficient of correlation (r), slope of the regression line (s), mean bias (in K) and RMSD (in K). The collocation pairs from entire granules are rejected if any of the following is true:
    - $r < 0.7$
    - $0.9 > s > 1.1$
    - Mean bias > 3 K
    - RMSD > 5 K
    - If outliers detected from previous test (MAD) are > 40% in the granule.

The collocation pairs for successfully passed from all these granules are combined for each day. This process was successfully tested for all INSAT-3D acquisitions with large geolocation errors and all INSAT-3D Imager and Sounder acquisitions as well as IASI granules having spurious data fields of radiances or zenith angles.

4.d. *Auxiliary Datasets*

It may be useful to incorporate land/sea/ice masks and/or cloud flags to allow analysis of statistics in terms of other geophysical variables – e.g. land/sea/ice, cloud cover, etc. All auxiliary data (land/sea/cloud cover) available from the products are retained with the collocation pair.

5. Monitoring

5.a. *Define Standard Radiances (Offline)*

This component provides standard reference scene radiances at which instruments' inter-calibration bias can be directly compared and conveniently expressed in units understandable by the users. Because biases can be scene-dependent, it is necessary to define channel-specific *standard radiances*. More than one standard radiance may be needed for different applications – e.g. clear/cloudy, day/night. This component is carried out offline.

A representative Region of Interest (RoI) is selected and histograms of the observed radiances within RoI are calculated for each channel. Histogram peaks are identified corresponding to clear/cloudy scenes to define standard radiances. These are determined *a priori* from representative sets of observations. The FoR is limited to within 30° latitude/longitude of the GEO sub-satellite point and times limited to night-time LEO overpasses.

5.a.i. INSAT-3D - IASI Specific:

Table-1 & 2 provides the reference temperature for all infrared channels from INSAT-3D Sounder & Imager, respectively. These values are computed from the mode of the histogram in the bins for 5K (for a few channels having bimodal distributions, the mean of the modes are used).

Table 1: INSAT-3D Sounder Channels Characteristics

Ch. No.	λ_c (μm)	ν_c (cm^{-1})	NEΔR ($mW/m^2/Sr/cm^{-1}$)	Ref. Temperature (K)
1	14.67	682	0.2900	215
2	14.31	699	0.2700	220
3	14.03	713	0.2600	245
4	13.64	733	0.2100	260
5	13.33	750	0.2100	275
6	12.59	794	0.1200	290
7	11.98	834	0.0900	295
8	10.99	910	0.0900	295
9	9.69	1032	0.1600	275
10	7.43	1346	0.0490	265
11	7.04	1421	0.0430	255
12	6.52	1534	0.0680	235
13	4.61	2168	0.0064	295
14	4.54	2202	0.0058	275
15	4.48	2232	0.0053	260
16	4.15	2408	0.0031	285
17	4.01	2496	0.0024	295
18	3.79	2642	0.0015	300

Table 2: INSAT-3D Imager Channels Characteristics

Ch. No.	λ_c (μm)	ν_c (cm^{-1})	NEΔR ($mW/m^2/Sr/cm^{-1}$)	Ref. Temperature (K)
3	3.93	2548.40	0.0108	300
4	6.88	1454.40	0.0298	250
5	10.83	925.09	0.1689	295
6	11.96	838.57	0.4370	295

5.b. *Regression of Most Recent Results*

Regression is used as the basis of the systematic comparison of collocated radiances from two instruments. (This comparison may also be done in counts or brightness temperature.) Regression coefficients shall be made available to users to apply the GSICS Correction to the target instrument, re-calibrating its radiances to be consistent with those of the reference instrument. Scatter plots of the regression data should also be produced to allow visualisation of the distribution of radiances.

The recommended approach is to perform a weighted linear regression of collocated radiances. The inverse of the sum of the spatial and temporal variance of the target radiance and the radiometric noise provide an estimated uncertainty on each dependent point, which is used as a weighting (Including the radiometric noise ensures that very homogeneous targets scenes where all the pixels give the same radiance do not have undue influence on the weighted regression.)

This method produces estimates of regression coefficients describing the slope and offset of the relationship between the two instruments' radiances – together with their uncertainties, expressed as a covariance. The problem of correlation between the uncertainties on each coefficient may be reduced by performing the regression on a transformed dataset – for example, by subtracting the mean or reference radiance from each set.

The observations of the reference instrument, x, and target instrument, y, are fitted to a straight line model of the form:

Equation 1: $\hat{y}(x) = a + bx$

We assume an uncertainty σ_i associated with each measurement, y_i, is known and that the dependent variable, x_i is also known.

To fit the observed data to the above model, we minimise the chi-square merit function:

Equation 2: $\chi^2(a,b) = \sum_{i=1}^{N} \left(\frac{y_i - a - bx_i}{\sigma_i} \right)^2$

This can be implemented following the method described in Section 15.2 of Numerical Recipes [Press *et al.*, 1996], which is implemented in the *POLY_FIT* function of IDL, yielding the following estimates of the regression coefficients:

Equation 3: $$a = \frac{\sum_{i=1}^{N}\frac{x_i^2}{\sigma_i^2}\sum_{i=1}^{N}\frac{y_i}{\sigma_i^2} - \sum_{i=1}^{N}\frac{x_i}{\sigma_i^2}\sum_{i=1}^{N}\frac{x_i\,y_i}{\sigma_i^2}}{\sum_{i=1}^{N}\frac{1}{\sigma_i^2}\sum_{i=1}^{N}\frac{x_i^2}{\sigma_i^2} - \left(\sum_{i=1}^{N}\frac{x_i}{\sigma_i^2}\right)^2},$$

Equation 4: $$b = \frac{\sum_{i=1}^{N}\frac{1}{\sigma_i^2}\sum_{i=1}^{N}\frac{x_i\,y_i}{\sigma_i^2} - \sum_{i=1}^{N}\frac{x_i}{\sigma_i^2}\sum_{i=1}^{N}\frac{y_i}{\sigma_i^2}}{\sum_{i=1}^{N}\frac{1}{\sigma_i^2}\sum_{i=1}^{N}\frac{x_i^2}{\sigma_i^2} - \left(\sum_{i=1}^{N}\frac{x_i}{\sigma_i^2}\right)^2},$$

their uncertainties:

Equation 5: $$\sigma_a^2 = \frac{\sum_{i=1}^{N}\frac{x_i^2}{\sigma_i^2}}{\sum_{i=1}^{N}\frac{1}{\sigma_i^2}\sum_{i=1}^{N}\frac{x_i^2}{\sigma_i^2} - \left(\sum_{i=1}^{N}\frac{x_i}{\sigma_i^2}\right)^2},$$

Equation 6: $$\sigma_b^2 = \frac{\sum_{i=1}^{N}\frac{1}{\sigma_i^2}}{\sum_{i=1}^{N}\frac{1}{\sigma_i^2}\sum_{i=1}^{N}\frac{x_i^2}{\sigma_i^2} - \left(\sum_{i=1}^{N}\frac{x_i}{\sigma_i^2}\right)^2},$$

and their covariance:

Equation 7: $$\mathrm{cov}(a,b) = \frac{-\sum_{i=1}^{N}\frac{x_i}{\sigma_i^2}}{\sum_{i=1}^{N}\frac{1}{\sigma_i^2}\sum_{i=1}^{N}\frac{x_i^2}{\sigma_i^2} - \left(\sum_{i=1}^{N}\frac{x_i}{\sigma_i^2}\right)^2}$$

5.b.i. INSAT-3D - IASI Specific

Radiometric noise of INSAT-3D Imager and Sounder channels are added to the scene variance in calculating the weighting for each point. The radiometric noise is calculated with blackbody observation data obtained from Lab-measurements or onboard noise computation. Noise values for each of INSAT-3D Imager and Sounder channels are provided in table-1& 2.

5.c. *Bias Calculation*

Inter-calibration biases should be directly comparable for representative scenes and conveniently expressed in units understandable by the users. Because biases can be scene-dependent, they are evaluated here at the standard radiances defined in 5.a.

General Options

Regression coefficients are applied to estimate expected bias, $\Delta\hat{y}(x_{REF})$, and uncertainty, $\sigma_{\hat{y}}(x_{REF})$, for standard radiances, accounting for correlation between regression coefficients.

Equation 8: $\Delta\hat{y}(x_{REF}) = a + bx_{REF} - x_{REF}$

Equation 9: $\sigma^2_{\hat{y}}(x_{REF}) = \sigma^2_a + \sigma^2_b x^2_{REF} + 2\,\mathrm{cov}(a,b)x_{REF}$

The results may be expressed in absolute/ % bias in radiance, or brightness temperature differences.

5.c.i. INSAT-3D - IASI Specific:

Biases and their uncertainties are converted from radiances to brightness temperatures for visualisation purposes.

5.d. *Consistency Test*

5.d.i. Purpose

The most recent results are tested for statistical consistency with the previous time series of results. Users should be alerted to any sudden changes in the calibration of the instruments, allowing them to investigate potential causes and *reset trend* statistics. The consistency test may be performed in terms of regression coefficients or biases.

The biases calculated for standard radiances from the most recent collocations are compared to the statistics of the biases' trends calculated from previous results. If the most recent result falls outside the 3σ (99.7%) confidence limits estimated from the trend statistics, an alert should be raised. This alert should trigger the Principle Investigator to check the cause of the change and reset the trends by issuing a *trend reset*.

5.d.ii. INSAT-3D - IASI Specific

Not implemented at present

5.e. *Trend Calculation*

It is important to establish whether an instrument's calibration is changing slowly with time. It is possible to establish this from a time-series of inter-comparisons by calculating a trend line using a linear regression with date as the independent variable. Only the portion of the time series since the most recent *trend reset* is analysed, to allow for step changes in the instruments' calibration.

The time series of biases evaluated at standard radiances can be regressed against the time (date) as the independent variable. The linear regression can be weighted by the calculated uncertainty on each bias. The regression coefficients including uncertainties (and their covariances) are calculated by the least squares method described. In this case, the variables, x_i and y_i are time series of Julian dates and radiance biases estimated for each orbit since the most recent *trend reset*, respectively.

5.e.i. INSAT-3D - IASI Specific

Not implemented at present.

5.f. *Define Smoothing Period (Offline)*

It is possible to combine data from a time series of inter-comparison results to reduce the random component of the uncertainty on the final GSICS Correction. However, this requires us to define representative periods over which the results can be smoothed without introducing bias due to calibration drifts during the smoothing period.

5.f.i. INSAT-3D - IASI Specific

At present it is empirically defined as 30 days. However, we need to investigate the natural variability of bias and revise smoothing period accordingly separately for INSAT-3D Imager and Sounder.

5.g. *Smooth Results*

It is possible to combine data from a time series of inter-comparison results to reduce the random component of the uncertainty on the final GSICS Correction. These smoothed coefficients provide the *Statistical Data* supplied in netCDF format files following the GSICS convention (https://gsics.nesdis.noaa.gov/wiki). The smoothing period defined in previous section is used.

5.g.i. INSAT-3D - IASI Specific

All the collocation data within the smoothing period (30 days) is combined and the regression [5.b] is repeated on the aggregate dataset. This approach ensures all data is used optimally, with appropriate weighting according to its estimated uncertainty. This is the recommended approach in general for GSICS.

6. INSAT-3D Re-Analysis Correction (RAC)

The reanalysis products are computed using the smoothing period of ±15 days, i.e. for the period t-15 to t+15 days, where t is the day when reanalysis product is generated.

References:

Blumstein, D., B. Tournier, F. R. Cayla, T. Phulpin, R. Fjortoft, C. Buil, and G. Ponce, 2007: In-flight performance of the infrared atmospheric sounding interferometer (IASI) on Metop-A, *Proc. SPIE*, **6684**, pp. 66840H-1–66840H-12.

Elloit, D., H. Aumann, L. Strow and S. Hannon, 2009: Two-year comparison of radiances from the Atmospheric Infrared Sounder (AIRS) and the Infrared Atmospheric Sounding Interferometer (IASI), *Proc. SPIE*, vol. 7456, pp. 75560S.

Hewison, T. J., X. Wu, F. Yu, Y. Tahara, X. Hu, D. Kim, and M. Koenig, 2013, GSICS Inter-Calibration of Infrared Channels of Geostationary Imagers Using Metop/IASI, *IEEE Trans. Geosci. Remote Sens.*, **51** (3), pp. 1160-1170.

Hewison, T.J., 2009: Quantifying the Impact of Scene Variability on Inter-Calibration, GSICS Quarterly, Vol. 3, No. 2, 2009.

Minnis, P., A. V. Gambheer, and D. R. Doelling, 2004: Azimuthal anisotropy of longwave and infrared window radiances from CERES TRMM and Terra data. *J. Geophys. Res.*, **109**, D08202, doi:10.1029/2003JD004471.

Pagano, T.S., H.H. Aymann, D.E. Hagan, and K. Overoye, 2003: Prelaunch and In-flight radiometric calibration of the Atmospheric Infrared Sounder (AIRS), *IEEE Trans. Geosci. Remote Sensing*, **41**, pp. 265-273.

Shukla, M. V., P. K. Thapliyal, J. H. Bisht, K. N. Mankad, P. K. Pal, and R. R. Navalgund, 2012: Intersatellite Calibration of Kalpana Thermal Infrared Channel Using AIRS Hyperspectral Observations, *IEEE Geosci. Rem. Sens. Letters*, **9 (4)**, 687-689. (doi: 10.1109/LGRS.2011.2178813).

Strow, L., S. Hannon, D. Tobin, and H. Revercomb, 2008: Intercalibration of the AIRS and IASI operational infrared sensors. *Proc. 17th Annual Conf. on Characterization and Radiometric Calibration for Remote Sensing (CALCON)*, Logan, UT, Utah State University Research Foundation.

Tahara, Y., and K. Kato, 2009: New Spectral Compensation Method for Intercalibration Using High Spectral Resolution Sounder, Meteorological Satellite Center Technical Note, No. 52, 1-37.

Tobin, D. C., H. E. Revercomb, C. C. Moeller, and T. Pagano, 2006: Use of Atmospheric Infrared Sounder high-spectral resolution spectra to assess the calibration of Moderate resolution Imaging Spectroradiometer on EOS Aqua, *J. Geophys. Res.*, **111**, D09S05, doi:10.1029/2005JD006095.

Tobin, D. C., H. E. Revercomb, F. Nagle, and R. Holz, 2008: Evaluation of IASI and AIRS spectral radiances using simultaneous nadir overpasses. *Proc. 16th Int. TOVS Study Conf.*, Angra dos Reis, Brazil, Int. TOVS Working Group. [Available online at http://cimss.ssec. wisc.edu/itwg/itsc/itsc16/posters/B07_dave_tobin.pdf.]

Wang, L., M. Goldberg, X. Wu, C. Cao, R. A. Iacovazzi, Jr., F. Yu, and Y. Li, 2011, Consistency assessment of AIRS and IASI radiances: Double differences versus simultaneous nadir overpasses," *J. Geophys. Res.*, **116 (**D11).

Wu, X., 2009: GSICS GOES-AIRS Inter-Calibration Algorithm at NOAA GPRC, Draft version dated January 5, 2009.

Wu, X., T. J. Hewison, and Y. Tahara, 2009, GSICS GEO-LEO inter-calibration: Baseline algorithm and early results, *Proc. SPIE*, **7456**, pp. 745604-1–745604-12.